Malaysian Journal of Analytical Sciences, Vol 22 No 4 (2018): 648 - 658
DOI: https://doi.org/10.17576/mjas-2018-2204-11

MALAYSIAN JOURNAL OF ANALYTICAL SCIENCES
Published by The Malaysian Analytical Sciences Society
ISSN 1394 - 2506

SYNERGISTIC EFFECT OF ADSORPTION-PHOTODEGRADATION OF COMPOSITE TiO_2/AC FOR DEGRADATION OF 1-BUTYL-3-METHYLIMIDAZOLIUM CHLORIDE

(Kesan Sinergistik Penjerapan-Fotopenguraian dari Bahan Komposit TiO_2/AC untuk Mengurai 1-Butil-3-Metillimidazolium Klorida)

Azhar Zawawi, Raihan Mahirah Ramli*, Noorfidza Yub Harun

Chemical Engineering Department,
Universiti Teknologi PETRONAS, 32610, Bandar Seri Iskandar, Perak, Malaysia

**Corresponding author: raihan.ramli@utp.edu.my*

Received: 16 April 2017; Accepted: 7 March 2018

Abstract

Most ionic liquids (ILs) were reported to be highly toxic and non-biodegradable such as ILs with imidazolium type cation. To overcome this problem, degradation of imidazolium based ILs via advance oxidation process is needed. In this research, photocatalytic study was employed in order to study the efficiency of the system for removal of ILs from wastewater. To introduce synergistic effect of adsorption-photodegradation, composite photocatalyst TiO_2/AC was synthesized using two steps (1) nano-TiO_2 was synthesized using microemulsion method and (2) it deposited onto functionalize (AC) activated carbon using impregnation method. The prepared composite photocatalyst was characterized using Thermo Gravimetric Analyzer (TGA), Brunauer-Emmet-Teller (BET) and Field Emission Scanning Electron Microscopic (FESEM). Photocatalytic study of 1-butyl-3-methylimidazolium chloride (bmimCl) was employed under visible light region. Increasing amount of AC as support increased the degradation rate of bmimCl. However, excess AC reduced the removal rate of bmimCl. Composite TiO_2/AC with 10 wt.% AC as support shows highest degradation rate with total removal 18.47%. Composite photocatalyst may enhance the diffusion rate between bmimCl and TiO_2 surface which increase the efficiency for overall systems.

Keywords: photodegradation, TiO_2, ionic liquid, activated carbon, synergistic

Abstrak

Penggunaan cecair ionik (ILs) dilaporkan sebagai sangat toksik dan tidak biodegradasi. Oleh itu, penguraian ILs dengan melalui proses pengoksidaan amat diperlukan. Dalam kajian ini, sistem fotopemangkin telah dilaksanakan untuk mengkaji kecekapan sistem ini dalam menyingkirkan ILs daripada air sisa. Komposit fotopemangkin TiO_2/AC telah dihasilkan untuk mencetuskan kesan sinergistik penjerapan-fotopenguraian untuk mengurai Ils melalui dua langkah (1) nano-TiO_2 telah dihasilkan melalui kaedah mikroemulsi dan (2) dicampurkan bersama karbon yang diaktifkan melalui kaedah pengisitepuan. Komposit fotopemangkin yang dihasilkan telah dihantar untuk proses pencirian bagi mengkaji ciri-ciri fizikal dan kimia fotopemangkin seperti analisis gravimetrik termo (TGA), Brenaeur-Emmet-Teller (BET) dan mikroskopi elektron pancaran medan (FESEM). Kajian fotopenguraian 1-butil-3-metilimidazolium klorida (bmimCl) sebagai rujukan ILs telah dilaksanakan di bawah sinar nampak. Penambahan bilangan AC sebagai sokongan telah meningkatkan kadar penguraian bmimCl. Walau bagaimanapun, sekiranya AC yang digunakan sebagai sokongan terlalu banyak, ianya telah mengurangkan kadar penguraian bmimCl. Komposit TiO_2/AC dengan bilangan 10 wt.% AC sebagai sokongan telah menunjukkan kadar penguraian yang paling tinggi. Komposit fotopemangkin akan meningkatkan kadar penyebaran antaran bmimCl and permukaan TiO_2 yang mana akan meningkatkan kecekapan sistem secara keseluruhannya.

Kata kunci: fotopenguraian, TiO_2, cecair ionik, karbon aktif, sinergistik

Introduction

Ionic liquids (ILs) have gained interest among researchers due to its tuneable properties that can be used in different application such as catalysis, separation and reaction processes [1]. ILs is regarded as a green solvent due to its negligible vapour pressure properties that can reduce the emission of chemicals to atmosphere. Imidazolium, quaternary ammonium and pyridinium are examples of cations that can be used to alter the physical and chemical properties of ILs [2] while halide groups (Cl^- and Br^-), tetrafluoroborate (BF_4^-) and tetracholoroaluminate ($AlCl_4^-$) are example of anions that have been used by researchers to tune the properties of ILs depending on its applications [1].

Aromatic ILs are known to be highly persistent in water, toxic and non-biodegradable. Advance oxidation processes (AOPs) such as electrochemical oxidation, Fenton systems and photocatalytic process under UV region [3-5] have been studied for removal of bmimCl from wastewater. Yet, there are several drawbacks of these systems such as high consumption of energy and formation of sludge. Photocatalytic process can be optimized by shifting the photoactivity of semiconductor towards the visible region since solar spectrum consist only 3-5% of UV region as compared to visible region up to 45% [6]. TiO_2 nanoparticles possess characteristics high photocatalytic activity, chemically stable and abundant [7]. However, major limitations of pristine TiO_2 that hinder its application in industry are high band gap energy and low diffusion rate between the targeted pollutant and TiO_2 surface [8, 9].

Nowadays, synthesis of nano-photocatalyst is mainly focusing on enhancing diffusion rate between pollutant and TiO_2 surface. Due to the hydrophilic nature of ILs, it is expected to diffuse slowly on TiO_2 surface, leading to low overall performance. The photodegradation study of bmimCl using TiO_2 as photocatalyst are still limited where based on the previous study, the research was mainly focusing on UV region as compared to visible region [10]. Hence, this study is focusing on the synthesis of activated carbon (AC) as support for TiO_2 with functionalize group to act as centre of accumulation. This process is to ensure high degradation rate of target pollutants onto TiO_2/AC surface leading to efficient overall system.

Materials and Methods

Materials

Titanium tetraisopropxide, TTIP ($C_{12}H_{28}O_4$, 97%), heptane (C_7H_{16}, 99%), hexanol ($C_6H_{14}O$, 98%), ferum nitrate nonahydrate ($Fe(NO_3)_3.9H_2O$), ethanol (C_2H_3OH, 95%) and 1-butyl-3-methylimidazolium chloride, bmimCl ($C_8H_{15}ClN_2$) were purchased from Merck (Germany). Triton X-100 ($C_{34}H_{62}O_{11}$, AR), nitric acid (HNO_3, 65%), potassium dihydrogen phosphate (KH_2PO_4) and triethylamine ($C_6H_{15}N$, AR) were purchased from R&M Chemicals (Malaysia). Meanwhile, phosphoric Acid (H_3PO_4, 85%) was purchased from QreC (New Zealand). All chemicals were used without further purification.

Methods

TiO_2 was prepared via microemulsion as reported from previous study [11]. Then, 1g of prepared TiO_2 was suspended in 10 ml of distilled water under continuous stirring. The solvent was removed at 80 $^{\circ}$C until white thick paste was formed. The resulting paste was dried in an oven at 80 $^{\circ}$C overnight prior to calcination at 400 $^{\circ}$C for 1.5 hours. Meanwhile, AC was prepared using bagasse as raw material and was carbonized in normal furnace at temperature 600 $^{\circ}$C for 1 hour. The produced biochar was then treated in a 1 M of nitric acid boiling solution. Then, resulting black powder was washed repeatedly with distilled water and dried in an oven for overnight at 80 $^{\circ}$C.

The synthesised TiO_2 was deposited onto AC using impregnation method. Pre-determined amount of TiO_2 and AC was mixed in a beaker and then 10 ml of distilled water was added. The mixture was stirred while heating until formation grey thick paste. The paste formed was dried overnight and then calcined at desired temperature. Samples are labelled following the format; TiO_2/nAC where n denotes the wt.% of AC i.e. TiO_2/5AC means 5wt.% of AC is used as support.

Characterization of photocatalyst

Synthesized photocatalyst were characterized using thermo gravimetric analysis (TGA) prior to calcination in order to determine the suitable temperature for calcination. The thermogram analysis was conducted using Perkin Elmer

TGA (Pyris 1) system under 20 ml/min N_2 flow, from 30–800 °C at ramp rate 20 °C /min. The morphology of photocatalyst was characterized using field emission scanning electron microscopic (FESEM) analysis. For FESEM analysis, model Zeiss Model Supra 35VP was used. Surface area and pore distribution was characterized using Brunauer-Emmet-Teller (BET) analysis. The characterization was done by using TriStar II 3020.

Photodegradation study

Photodegradation study was conducted in glass reactor at ambient condition. The reactor was placed under 500W halogen lamp with distance 15 cm. The initial concentration of bmimCl used was 5mM and 1g/L photocatalyst. The reactor was placed in dark for 30 minutes to allow for adsorption-desorption equilibrium prior to 4 hours photoreaction. The samples were analysed using Agilent 1100 high performance liquid chromatography (HPLC). Column used was Symmetry C-18 (250 x 4.6mm, 5µm) and mobile phase mixture of methanol (35 vol%) and 25 mM of phosphate buffer (KH_2PO_4/H_3PO_4) containing 0.5% of triethylamine were used to separate bmimCl. The analysis was conducted using injection 5 µl, temperature 30 °C and flow rate 0.8ml/min. UV detector with wavelength 212 nm was used to trace the BmimCl.

Results and Discussion

Thermo gravimetric analyser

Thermo gravimetric analyser (TGA) analysis was conducted to determine the thermal decomposition of the synthesized photocatalyst. From Figure 1(a), thermogram for TiO_2 shows significant weight loss from temperature 30-400 °C before the curve becomes constant. The significance weight loss may be due to loss of water from surface of sample and also elimination unhydrolyzed isopropoxide ligand as well as decomposition of organic entities that may present during synthesis steps [12, 13]. The derivative weight loss shows that the removal of water and organic entities from samples of photocatalyst was attributed by endothermic reaction.

Figure 1(b) shows the thermogram recorded for AC, the weight of compound increases from temperature 30 °C up to 500 °C. This is happened due to adsorption of N_2 gas at higher temperature to the surface of AC [14]. This is in agreement with finding reported by Kim et. al where AC has affinity towards adsorption of N_2[15]. At temperature 470 °C, the sample weight loss starts to decrease until 0.0 wt.% weight loss recorded at temperature 646 °C. This weight loss was due to the burning off the AC by endothermic process [16]. Figure 1(c) represent thermogram for TiO_2/AC where two significant weight losses recorded from temperature 30-400 °C (step 1) and 400-800 °C (step 2). Step 1 occurred due to endothermic reaction where the evaporation of adsorbed water vapour occurred at this temperature with main peak at 31°C. Second weight loss also occurred due endothermic reaction with broader main peak at 611°C.

Step 2 weight loss was due to the burn off the AC and only 15.4% weight loss was recorded compared to AC alone. The lower weight loss recorded was due to thermal persistent of composite photocatalyst containing synthesis TiO_2 at higher temperature [17]. Comparing to Figure 1(b), the increase in weight % due to adsorption of N_2 gas is not recorded for sample TiO_2/AC. This shows that the adsorption of N_2 gas during calcination treatment for composite photocatalyst did not occurred. From the previous study, adsorption of N_2 towards TiO_2 surface can only be done by specific complex cluster TiO_2 namely unsaturated Ti atom at the (110) surface of TiO_2. Hence due to specific formation of TiO_2 that can only adsorb N_2, the weight gain does not record in thermogram as negligible N_2 has been adsorbed during TGA analysis. From this finding also, we can conclude that synthesize bare TiO_2 and composite TiO_2/AC does not contain specific facets of TiO_2 that can be used to adsorb N_2 [18].

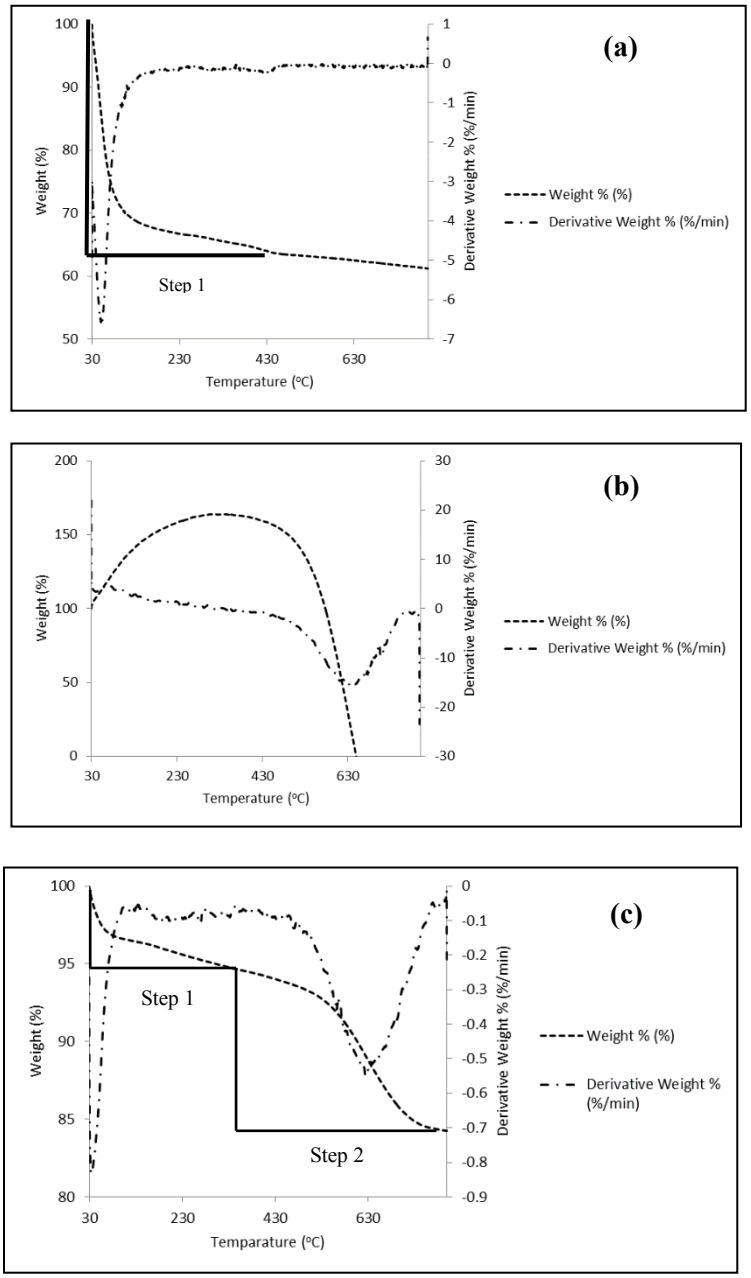

Figure 1. Thermogram analysis for (a) TiO_2, (b) AC and (c) TiO_2/AC

Surface area and pore distribution analyser

Figure 2 depicts the N_2 adsorption isotherms for TiO_2, AC and composite TiO_2/AC. TiO_2 and TiO_2/AC shows similar type of N_2 isotherm with type IV isotherm and hysteresis loop H3 type (Figure 2(a) and (c), respectively) meanwhile AC shows type I isotherm and hysteresis H4 type (Figure 2(b)) [16, 19]. TiO_2 and TiO_2/AC show a higher adsorption at relative P/P_o = 0.6-1.0 indicating the presence of mesoporous structure. The hysteresis loop was recorded due to aggregation of nanoparticles and this type of isotherm corresponds to lower porosity of material [20]. This phenomenon in agreement with BET surface area, (100.53 m^2/g). For AC, the adsorption uptake of N_2 occurring at pressure less than 0.1, followed by plateau at P/P_o more than 0.2 and indicating the microporosity of

AC. The hysteresis loops also confirm the presents of some mesoporous structure [16]. The pore distribution of TiO_2 and TiO_2/AC mainly distribute between 1.5-15.0 nm in agreement with isotherm result indicates the presence of microporous and mesoporous structure. Compare to TiO_2, AC pore volume distribute mainly around 1.5-2.0 nm represent the microporous structure of the sample [20].

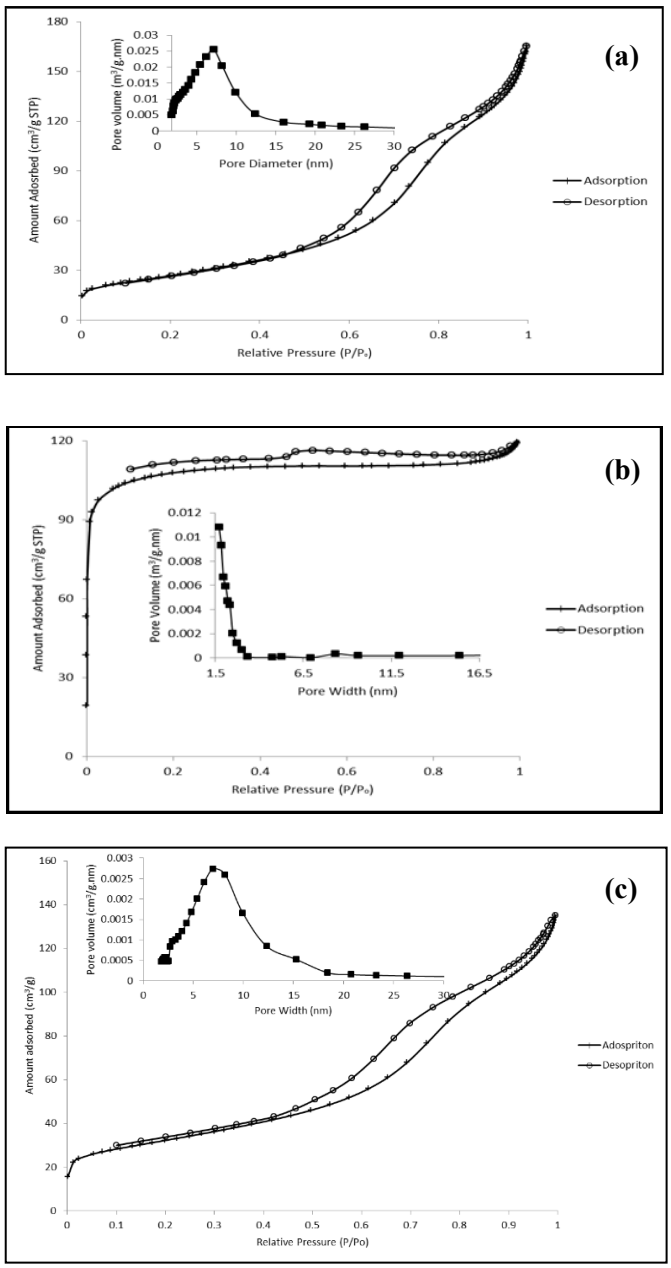

Figure 2. N_2 isotherm and pore distribution (inner graph) for (a) TiO_2, (b) AC and (c) TiO_2/10AC

Table 1 summarizes the surface area and pore size of synthesis TiO_2 and AC. From the table, it shows that AC has high surface area compared to synthesis TiO_2 and composite TiO_2/AC as AC was known to be highly surface area and porous structure. Reduction in surface area for composite photocatalyst compared to AC is mainly due to

blocking of the pores by TiO_2 that had been deposited on AC [16]. Interestingly, the V_{total} and pore size of the TiO_2 and composite photocatalyst is higher compared to synthesis AC and may lead to higher degradation rate of bmimCl. This is due to more adsorbate can be adsorbed in the pore structure of photocatalyst and enhance the diffusion rate between bmimCl and TiO_2 surface. This shows that synthesis TiO_2 via microemulsion produce highly porous structure of nanoparticles

Table 1. Specific surface area and pore diameters for the photocatalyst sample

Sample	S_{BET} (m^2/g)	V_{total} (cm^3/g)	Pore diameter (nm)
TiO_2	100.53	0.26	10.13
AC	335.25	0.18	7.98
TiO_2/10AC	96.29	0.21	8.67
TiO_2/20AC	111.97	0.20	7.28

Surface morphology

Morphological analysis was conducted using FESEM to investigate the surface structure of the samples. Micrographs in Figure 3 represent the imaging morphology for TiO_2, AC, TiO_2/10AC and TiO_2/20AC. AC image (Figure 2a) shows its spongy and porous structure similar to the report [21]. This is attributed to its high BET surface area (Table 1). While, the synthesized TiO_2 shows uniform spherical structure with particles size range between 15-18.00 nm, proving that the synthesis method produce small particle with high surface area as compared to commercialize TiO_2 P25 [22]. The spherical shape of TiO_2 provided higher surface area for photocatalyst that can be used to optimize the adsorption and absorption process which then enhance the degradation rate of ILs. The morphological of TiO_2 on surface of AC almost similar with morphology recorded for TiO_2 alone. In same time, agglomeration effect also could be observed from micrograph, with finer particles size could be observed for TiO_2 deposited onto AC (Figure 2c and d). This finding in agreement with discussion reported by Slimen et. al [23] where AC contain interfacial energy which can enhance and produce fine particle size of TiO_2. This theory was also supported by other researcher [19, 21].

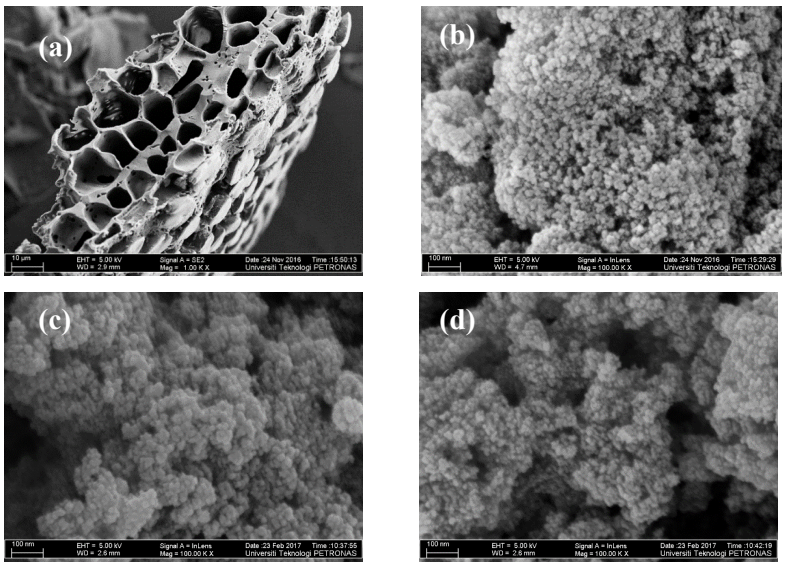

Figure 3. Imaging surface morphology of (a) AC (5 kX), (b) TiO_2 (100kX), (c) TiO_2/ 10AC (100kX) and (d) TiO_2/20AC (100kX)

Photodegradation analysis

Figure 4(a) depicts the concentration profile for AC treated with different type of acid. From the figure, the concentration of bmimCl started to increase after 30 minutes of adsorption study. Hence from this preliminary study, 30 minutes of dark reaction was selected prior to photodegradation under visible light to achieve equilibrium adsorption-photodegradation. Meanwhile Figure 4(b) shows the concentration profile for photodegradation process. From the figure, it shows that the concentration profile becomes plateau after 2 hours reaction. Based on the analysis, the photodegradation study will be done in 2 hours analysis for future study. Figure 4(c) presents the efficiency of bmimCl photodegradation process in different system and photocatalyst. In the photolysis process, bmimCl could not undergo self-destruction under visible light without the presence of photocatalyst. Meanwhile, the synthesized TiO_2 recorded 12% removal of bmimCl. However, significant increment of the photodegradation % was observed when the TiO_2 was deposited onto AC, with the highest removal was observed for 10 wt.% AC. When the amount of AC increase, total surface-active sites containing functionalized group increases and more interaction Van der Walls forces will occur between bmimCl and surface of AC [24]. Hence more bmimCl will be adsorbed on surface of AC and leading to increment in diffusion rate between bmimCl and surface of TiO_2. Hence direct oxidation of bmimCl occurred and increase in total degradation [25]. Compared to 5 wt.% of AC, the total removal of bmimCl was quite low. This is because, when less AC was used as support, the total surface of AC itself was blocked by TiO_2 leading to low active surface area which can be used to adsorb bmimCl. Moreover, generation of hydroxyl radical ($OH^{\bullet}$) as attacking agent in degradation study accumulate around surface of TiO_2. Production of $OH^{\bullet}$ can penetrate up to sub-millimeter distance from surface TiO_2. Interestingly, this radical also can penetrate into pore of AC to attack the pollutant that has been adsorbed deep into pore of AC. Hence, as bmimCl was accumulated on surface of AC, the molecules can be directly oxidized by $OH^{\bullet}$ thus increase the overall efficiency of the system [26].

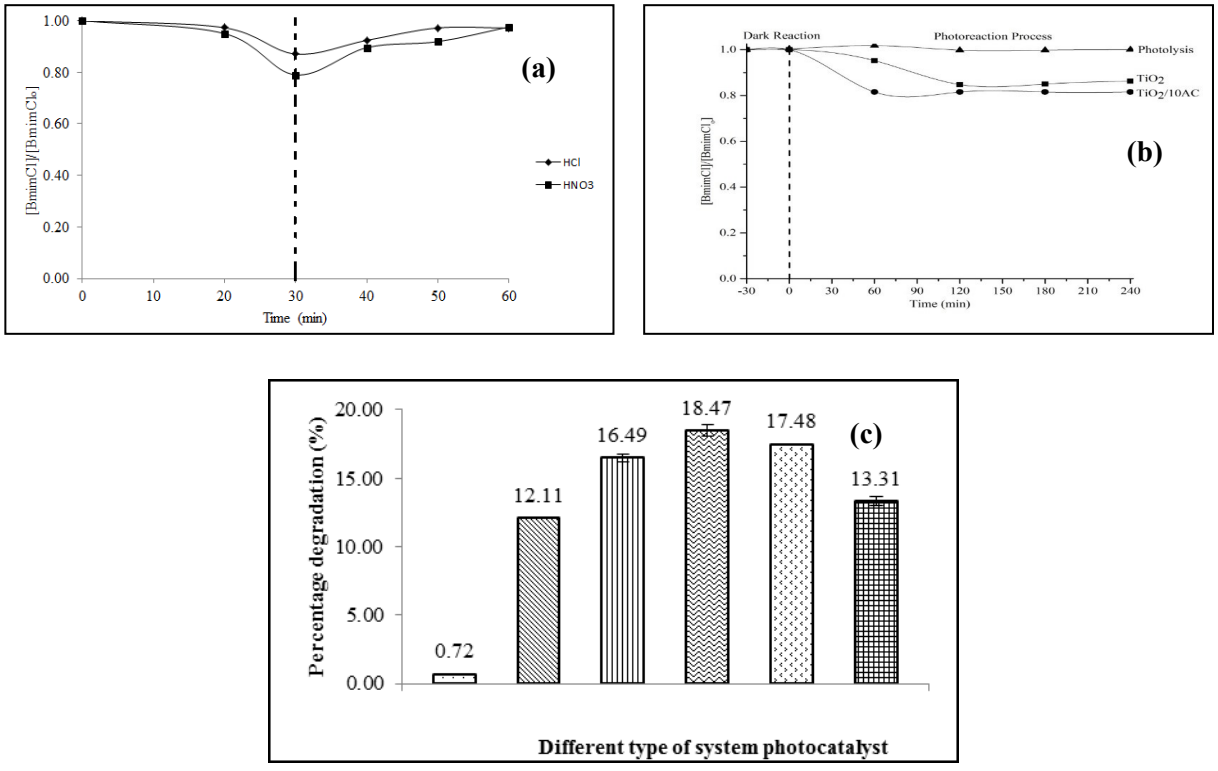

Figure 4. (a) Concentration profile for adsorption study of different type of AC, (b) concentration profile for photoreaction and (c) comparison photodegradation study for different type of photocatalyst

On the other hand, bare AC has been proved able to produce high water contact angle and leading to hydrophobic properties of AC. However, once AC was coated with TiO_2, the properties can be shifted to hydrophilic [27]. Hydrophilic composite materials could lead to increment in adsorption of organic molecule such as methylene blue (MB) [27] and Rhodamine-B [28] due to increase in the interaction of composite materials and targeted molecule itself. Hence degradation rate could increase.

The degradation reduced significantly when AC loading was increased from 10 to 20 wt.%. When the amount of AC used as support increased, more active site will be available for adsorption of bmimCl. Hence more bmimCl molecule will be accumulated on surface of AC. This phenomenon unfortunately, will block surface of TiO_2 and prevent the surface of TiO_2 from harvesting the light. Hence less charge carrier (e^-_{CB}/h^+_{VB}) could be generated and reduced the degradation rate. Similar phenomenon was recorded by other researchers [29]. In same time, TiO_2/20AC contains leas amount of TiO_2 based on synthesized procedure. Reduction in amount TiO_2 will reduce the active site TiO_2 surface that could be used to absorb photon for generation of charge carrier. Hence, less bmimCl molecule can be oxidized leading to reduction in total degradation rate.

The comparison of different types of AOP for degradation of ILs is presented in Table 2. From the table, all systems i.e. electrochemical oxidation, Fenton's oxidation and UV/TiO_2 systems show high degradation rate as compared to our current findings where only 18.47% total removal of bmimCl was recorded. The current finding is only focusing on the optimization of material development. The optimization of extrinsic factors such as initial pH of the solution, initial concentration of bmimCl, dosage of photocatalyst and the presence of oxidant are yet to be investigated. Apart from the optimization of material development, these factors also contribute significantly to the overall efficiency of the system [30]. In addition, major limitation of electrochemical oxidation is the dependency on electricity which relatively contributes to higher cost [31].

Table 2. Comparison study of AOP for degradation of ILs

AOP systems	Methodology	Findings	Ref.
Electrochemical Oxidation	Reaction run in electrolytic cell V = 100 ml, BDD as anode and stainless steel as cathode. Area and distance of electrode are 10 cm^2 and 1 cm respectively. Concentration of IL is 50 mg/l	100% of IL can be degrading in 120 minutes with optimum pH 3 and pH 6. Temperature of reactions was maintained at 40 °C. Degradation affected by IL used and imidazolium is more stable compare to pyridinium	[33, 34]
Fenton systems	Reaction run in reactor V = 300 ml, pH 3.5 and temperature maintained at 25 °C. Concentration of IL is 1.0 mM	IL with 100% degradation achieved in 60 minutes with presents of scavenger, [H_2O_2] = 400 mM and [Fe^{3+}] = 1 mM	[35-37]
UV/TiO_2 systems	Reactions run with 0.5 g/L of TiO_2 with 1 mM of IL and 1000 W Xenon arc lamp as light source	Almost 100% degradation can be achieved in 360 minutes	[10, 38]
TiO_2/AC	Reaction with 1g/L of TiO_2/AC with 5 mM of IL and 500W of Halogen lamp was used as source of light	Only 18.47% removal of bmimCl was achieved in 4 hours reactions without optimization of extrinsic factors	This study

On the other hand, the homogeneous nature of this process leads to the formation of ferric sludge during post-treatment prior to discharge which could cause another problem to the landfill management [32]. Though UV/TiO_2

system could be the solution to the problem faced by Fenton's oxidation process, limited capability of TiO_2 to adsorb visible light energy is not favoured since the solar spectrum consists only 4-5% of UV region as compared to visible region which is up to 45% [11]. The current finding shows the high potential of TiO_2/AC as photocatalyst to degrade bmimCl under visible light radiation, and provide options to overcome the limitation faced by the previously discussed processes. Further optimization work is anticipated to improve the overall efficiency of this photocatalytic system.

Conclusion

Degradation rate of bmimCl can be enhanced by employing activated carbon (AC) as the support for titania via the synergistic effect of adsorption-photodegradation of both materials. Positive effect of increasing AC amount further enhanced the diffusion rate of bmimCl from fluid phase to the surface of titania leading to direct oxidation of bmimCl by the titania. Optimum AC was found at 10 wt.% functionalized with 1M HNO_3 with maximum bmimCl removal of 18.47%. The synergistic effect of adsorption-photodegradation includes: (1) Interfacial energy on AC surface could prevent the transformation of anatase TiO_2 to rutile phase leading to the production of fine particle size. Hence more TiO_2 active site is available for the absorption of photon for generation of charge carrier, (2) functionalized group on AC could act as pollutant concentrator and enhanced the diffusion rate between bmimCl and TiO_2 surface leading to direct oxidation of bmimCl and (3) coating of TiO_2 with AC could shift the polarity of bare AC to become hydrophilic. This property then leads to the increase of interaction between composite materials and bmimCl and consequently increase the adsorption process. Hence more bmimCl can be directly oxidized by TiO_2.

Acknowledgement

Authors are grateful to Universiti Teknologi PETRONAS (UTP) for the research funding under I-Gen Grant (IGEN 0153 DA-162). Special thanks to Centralize Analytical Laboratory (CAL), UTP for the characterization analysis.

References

1. Olivier-Bourbigou, H., Magna, L. and Morvan, D. (2010). Ionic liquids and catalysis: Recent progress from knowledge to applications. *Applied Catalysis A: General,* 373(1-2): 1-56.
2. Pham, T. P., Cho, C. W. and Yun, Y. S. (2010). Environmental fate and toxicity of ionic liquids: A review. *Water Research,* 44(2): 352-372.
3. Siedlecka, E. M., Fabiańska, A., Stolte, S., Nienstedt, A., Ossowski, T., Stepnowski P. and Thöming, J. (2013). Electrocatalytic oxidation of 1-butyl-3-methylimidazolium chloride: Effect of the electrode material. *International Journal of Electrochemical Science,* 8(1): 5560-5574.
4. Munoz, M., Domínguez, C. M., de Pedro, Z. M., Quintanilla, A., Casas, J. A. and Rodriguez, J. J. (2015). Ionic liquids breakdown by fenton oxidation. *Catalysis Today,* 240(1): 16-21.
5. Zhou, H., Shen, Y., Lv, P., Wang, J. and Li, P. (2015). Degradation pathway and kinetics of 1-alkyl-3-methylimidazolium bromides oxidation in an ultrasonic nanoscale zero-valent iron/hydrogen peroxide system. *Journal of Hazardous Materials,* 284(1): 241-252.
6. Ramli, R. M., Chong, F. K. and Omar, A. A. (2013). Visible-light photodegradation of diisopropanolamine using bimetallic Cu-Fe/TiO_2 photocatalyst. *Advanced Materials Research,* 176(1): 451-458.
7. Saepurahman, Abdullah, M. A. and Chong, F. K. (2010). Preparation and characterization of tungsten-loaded titanium dioxide photocatalyst for enhanced dye degradation. *Journal of Hazardous Materials,* 176(1-3): 451-458.
8. Ramli, R. M., Kait, C. F. and Omar, A. A. (2014). Photodegradation of aqueous diisopropanolamine using Cu/TiO_2: Effect of calcination temperature and duration. *Applied Mechanics and Materials,* 625(1): 847-850.
9. Orha, C., Pode, R., Manea, F., Lazau, C. and Bandas, C. (2017). Titanium dioxide-modified activated carbon for advanced drinking water treatment. *Process Safety and Environmental Protection,* 108(1): 26-33.
10. Stepnowski, P., & Zaleska, A. (2005). Comparison of different advanced oxidation processes for the degradation of room temperature ionic liquids. *Journal of Photochemistry and Photobiology A: Chemistry,* 170(1): 45-50.
11. Ramli, R. M., Kait, C. F. and Omar, A. A. (2016). Remediation of DIPA contaminated wastewater using visible light active bimetallic Cu-Fe/TiO2 photocatalyst. *Procedia Engineering,* 148(1): 508-515.

12. Altın, İ., Sökmen, M. and Bıyıklıoğlu, Z. (2016). Sol gel synthesis of cobalt doped TiO_2 and its dye sensitization for efficient pollutant removal. *Materials Science in Semiconductor Processing,* 45(1): 36-44.
13. Mohd Zaid, H. F., Chong, F. K. and Abdul Mutalib, M. I. (2015). Photooxidative–extractive deep desulfurization of diesel using Cu–Fe/TiO_2 and eutectic ionic liquid. *Fuel,* 156(1): 54-62.
14. Al-Doghachi, F. A. J., Rashid, U. and Taufiq-Yap Y. H. (2016). Investigation of Ce(III) promoter effects on the tri-metallic Pt, Pd, Ni/MgO catalyst in dry-reforming of methane. *RSC Advances,* 6(1): 10372-10384.
15. Ho Kim, B., Reon Kim, B. and Seo, Y. G. (2005). A study on adsorption equilibrium for oxygen and nitrogen into carbon nanotubes. *Adsorption,* 11(1): 207-212.
16. Ouzzine, M., Romero-Anaya, A. J., Lillo-Ródenas, M. A. and Linares-Solano, A. (2014). Spherical activated carbon as an enhanced support for TiO_2/AC photocatalysts. *Carbon,* 67(1): 104-118.
17. Ganesh, I., Kumar, P. P., Annapoorna, I., Sumliner, J. M., Ramakrishna, M., Hebalkar, N. Y., Padmanabham, G. and Sundararajan, G. (2014). Preparation and characterization of Cu-Doped TiO_2 materials for electrochemical, photoelectrochemical, and photocatalytic applications. *Applied Surface Science,* 293(1): 229-247.
18. Rittner, F., Boddenberg, B., Fink, R. F. and Staemmler, V. (1999). Adsorption of nitrogen on rutile(110). 2. construction of a full five-dimensional potential energy surface. *Langmuir,* 15(4): 1449-1455.
19. Eliyas, A., Ljutzkanov, L., Stambolova, I., Blaskov, V., Vassilev, S., Razkazova-Velkova, E. and Mehandjiev, D. (2013). Visible light photocatalytic activity of TiO_2 deposited on activated carbon. *Open Chemistry,* 11(3): 464-470.
20. Xing, B., Shi, C., Zhang, C., Yi, G., Chen, L., Guo, H., Huang, G. and Cao, J. (2016). Preparation of TiO_2/activated carbon composites for photocatalytic degradation of RhB under UV light irradiation. *Journal of Nanomaterials,* 2016(1): 1-10.
21. Jamil, T. S., Ghaly, M. Y., Fathy, N. A., Abd el-halim, T. A. and Österlund, L. (2012). Enhancement of TiO_2 behavior on photocatalytic oxidation of MO dye using TiO_2/AC under visible irradiation and sunlight radiation. *Separation and Purification Technology,* 98(1): 270-279.
22. Raj, K. J. A. and Viswanathan, B. (2009). Effect of surface area, pore volume and particle size of P25 titania on the phase transformation of anatase to rutile. *Indian Journal of Chemistry,* 48(10): 1378-1382.
23. Slimen, H., Houas, A. and Nogier, J. P. (2011). Elaboration of stable anatase TiO_2 through activated carbon addition with high photocatalytic activity under visible light. *Journal of Photochemistry and Photobiology A: Chemistry,* 221(1): 13-21.
24. Lemus, J., Neves, C. M. S. S., Marques, C. F. C., Freire, M. G., Coutinho, J. A. P. and Palomar, J. (2013). Composition and structural effects on the adsorption of ionic liquids onto activated carbon. *Environmental Science: Processes & Impacts,* 15(9): 1752-1759.
25. Maneerung, T., Liew, J., Dai, Y., Kawi, S., Chong, C. and Wang, C. H. (2016). Activated carbon derived from carbon residue from biomass gasification and its application for dye adsorption: Kinetics, isotherms and thermodynamic studies. *Bioresource Technology,* 200(1): 350-359.
26. Huang, D., Miyamoto, Y., Matsumoto, T., Tojo, T., Fan, T., Ding, J., Guo, Q. and Zhang, D. (2011). Preparation and characterization of high-surface-area TiO_2/activated carbon by low-temperature impregnation. *Separation and Purification Technology,* 78(1): 9-15.
27. Zhou, W., Zhang, P. and Liu, W. (2012). Anatase TiO_2 nanospindle/activated carbon (AC) composite photocatalysts with enhanced activity in removal of organic contaminant. *International Journal of Photoenergy,* 2012: 1-7.
28. Li, Y., Zhou, X., Chen, W., Li, L., Zen, M., Qin, S. and Sun, S. (2012). Photodecolorization of Rhodamine B on tungsten-doped TiO_2/activated carbon under visible-light irradiation. *Journal of Hazardous Materials,* 227-228 (1): 25-33.
29. Sun, Z., He, X., Du, J. and Gong, W. (2016). Synergistic effect of photocatalysis and adsorption of nano-TiO_2 self-assembled onto sulfanyl/activated carbon composite. *Environmental Science and Pollution Research,* 23(21): 21733-21740.
30. Alkaim, A. F., Kandiel, T. A., Hussein, F. H., Dillert, R. and Bahnemann, D. W. (2013). Enhancing the photocatalytic activity of TiO_2 by pH Control: A case study for the degradation of EDTA. *Catalysis Science & Technology,* 3 (12): 3216-3222.
31. Siedlecka, E. M., Fabiańska, A., Stolte, S., Nienstedt, A., Ossowski, T., Stepnowski P. and Thöming, J. (2013). Electrocatalytic oxidation of 1-butyl-3-methylimidazolium chloride: Effect of the electrode material. *International Journal of Electrochemical Science,* 8(1): 5560-5574.

32. Ramli, R. M., Kait, C. F. and Omar, A. A. (2014). Photocatalytic degradation of diisopropanolamine in heterogeneous photo-fenton system. *Advanced Materials Research,* 917(1): 160-167.
33. Pieczyńska, A., Ofiarska, A., Borzyszkowska, A. F., Białk-Bielińska, A., Stepnowski, P., Stolte, S. and Siedlecka, E. M. (2015). A comparative study of electrochemical degradation of imidazolium and pyridinium ionic liquids: A reaction pathway and ecotoxicity evaluation. *Separation and Purification Technology,* 156 (Part 2): 522-534.
34. Fabiańska, A., Ossowski, T., Bogdanowicz, R., Czupryniak, J., Gnyba, M., Odzga, T., Janssens, S. D., Haenen, K. and Siedlecka, E. M. (2012). Electrochemical oxidation of ionic liquids at highly boron doped diamond electrodes. *Physica Status Solidi (A),* 209(9): 1797-1803.
35. Siedlecka, E. M., Gołębiowski, M., Kaczyński, Z., Czupryniak, J., Ossowski, T. and Stepnowski, P. (2009). Degradation of ionic liquids by fenton reaction; The effect of anions as counter and background ions. *Applied Catalysis B: Environmental,* 91(1-2): 573-579.
36. Siedlecka, E. M., Mrozik, W., Kaczyński, Z. and Stepnowski, P. (2008). Degradation of 1-butyl-3-methylimidazolium chloride ionic liquid in a fenton-like system. *Journal of Hazardous Materials,* 154(1): 893-900.
37. Siedlecka, E. M., Goêbiowski, M., Kumirska, J. and Stepnowski, P. (2008). Identification of 1-butyl-3-methylimidazolium chloride degradation products formed in Fe(III)/H_2O_2 oxidation system. *Journal of Analytical Chemistry,* 53(1): 943-951.
38. Czerwicka, M., Stolte, S., Müller, A., Siedlecka, E. M., Gołębiowski, M., Kumirska, J. and Stepnowski, P. (2009). Identification of ionic liquid breakdown products in an advanced oxidation system. *Journal of Hazardous Materials,* 171(1): 478-483.